INTERNATIONAL JOURNAL OF
NUMERICAL ANALYSIS AND MODELING
Volume 19, Number 4, Pages 439–457

A FINITE DIFFERENCE METHOD FOR ELLIPTIC PROBLEMS WITH IMPLICIT JUMP CONDITION

FUJUN CAO, DONGFANG YUAN, ZHIQIANG SHENG, GUANGWEI YUAN*, AND LIMIN HE

Abstract. In this paper linear elliptic problems with imperfect contact interface are considered, and a second order finite difference method is presented for linear problems, in which implicit jump condition are imposed on the interface. Then, the stability and convergence analysis of the FD scheme are given for the one-dimensional elliptic interface problem. Numerical examples are carried out for the elliptic problems with imperfect contact interfaces, and the results demonstrate that the scheme has second order accuracy for elliptic interface problems of implicit jump conditions with single and multiple imperfect interfaces.

Key words. Implicit jump conditions, elliptic interface problem, imperfect contact.

1. Introduction

Interface problems occur in many multi-physics and multi-phase applications in science and engineering, particularly for free boundary/moving interface problems, for examples, the modeling of the Stefan problem of solidification process and crystal growth, composite materials, multi-phase flows, cell and bubble deformation, and many others. To be simple to expression, we consider the interface problems in multi-material heat transfer process. According to the different jump conditions, the interface problems can be divided into two main categories: (1) Perfect contact, that is, the contact between the two objects is perfect, which means that the temperature and normal heat flux are continuous on the interface. (2) Imperfect contact, for example, there are weakly conductive thin films or interlayers between the two objects, so that temperature or normal heat flux is discontinuous across the interface. In practice, an equivalent boundary condition is often presented on the thin layer, namely the interface jump (or connection) condition. When the contact interface is not perfect, the jump condition on the interface can be roughly divided into the following classes.

(1) The first class of imperfect interface condition is that jump sizes are given [15, 16, 17, 21, 22], which can be named as explicit jump condition for the sake of convenience and are shown as follows:

$$\begin{cases} [u] = u^+ - u^- = h_1(x), \quad \text{on} \quad \Gamma, \\ [\kappa \frac{\partial u}{\partial \vec{n}}] = \kappa^+ \frac{\partial u^+}{\partial \vec{n}} - \kappa^- \frac{\partial u^-}{\partial \vec{n}} = h_2(x), \quad \text{on} \quad \Gamma, \end{cases} \tag{1}$$

where $h_1(x)$ and $h_2(x)$ are given functions.

(2) The second class of imperfect interface condition is that the jump size of temperature is proportioned to flux, which can be named as implicit jump condition

Received by the editors March 1, 2021 and, in revised form, August 22, 2021.
2000 *Mathematics Subject Classification.* 35R35, 49J40, 60G40.
*Corresponding author.

and be written in the following form [1, 2, 3, 9, 11, 12, 36, 58]

$$\begin{cases} [u] = u^+ - u^- = \lambda\kappa^- \frac{\partial u^-}{\partial \vec{n}}, \quad \text{on} \quad \Gamma, \\ [\kappa \frac{\partial u}{\partial \vec{n}}] = \kappa^+ \frac{\partial u^+}{\partial \vec{n}} - \kappa^- \frac{\partial u^-}{\partial \vec{n}} = 0, \quad \text{on} \quad \Gamma, \end{cases} \tag{2}$$

where Γ is a curve which divides the region Ω into two non-intersected subregions Ω^+ and Ω^-, $\Omega = \Omega^- \cup \Omega^+ \cup \Gamma$. $\vec{n}$ is the outer unit normal vector of the interface Γ in Ω^-. κ^- and κ^+ represent the material conduction coefficients on Ω^- and Ω^+, respectively.

In this paper we consider the problems with the interface conditions, where the jumps of temperature are related to the normal heat fluxes. The second class implicit connection condition of the imperfect interface can be used to describe the heat conduction problem of two objects with imperfect contact [1]. If there is a interlayer with thickness δ and the thermal conductivity is ϵ between two objects, and when $\delta \to 0$, $\epsilon/\delta \to const = \lambda$, then the interlayer is degenerated into a sharp interface. In the implicit jump conditions, the jumps of physical quantities are unknown and proportional to the flux across the interface. The implicit connection condition has a clear physical meaning. Moreover, it can be used to describe the problem of temperature discontinuity between gas and cooling solid surface [4]. In addition, it is appeared in some other applications, such as the effective thermal conductivity of composite materials [5], the dielectric heat conduction problem of solid spherical particles dispersed in the continuous phase [6], the interface problem with thermal resistance between the composite and the discrete components [7]. In the problem of steady thermal diffusion in a two component nonhomogeneous conductor with contact resistance, the flow of heat through the material interface is also considered to be proportional to the jump of the temperature field [9, 10, 13]. The solution to an imperfect interface problem, therefore, typically is non-smooth or even discontinuous across the interfaces. It is necessary to study accurate and robust numerical methods for these elliptic interface problems.

When the jump sizes along the interface are known explicitly, (say $[u] = h_1$, $[\kappa\partial u/\partial\vec{n}] = h_2$, with given h_1 and h_2), there are various numerical approaches, such as immersed interface method (IIM) [15, 16, 17, 19, 20, 23], immersed finite volume method (IFVM) [24, 25, 26] and immersed finite element (IFE) methods [27, 28, 30, 31, 34, 37, 38, 45, 56], and they are presented to effectively handle the explicit jump conditions. Since the pioneer work by [15], the immersed interface method (IIM) has becoming increasingly popular for elliptic interface problems. The original IIM achieve uniformly second order accuracy, and a key feature is that computational stencils for irregular points are modified such that the information on the boundary is used exactly where grid lines intersect the immersed boundary. Recently, there have been many further developments and analysis in various aspects of the immersed interface methods [16, 17, 19, 21, 22]. Among these developments, Li and Ito [17] constructed a fourth-order accurate finite difference method for interface problems which produces a large sparse linear system with M-matrix in several-dimensions and is coupled with a multigrid solver achieving fast convergence of the linear solver. Wiegmann and Bube [21] developed an explicit-jump immersed interface method for some special cases, where the explicit jump conditions of physical quantity and its derivatives ($[u]$, $[u_x]$, $[u_{xx}]$, etc.) are known. Mittal et al. [23] use standard finite difference formulas at grid points near the interface using interfacial points also as one of the nodes and the Lagrange polynomial interpolation is then used to find the unknown values at interfacial points. The proposed scheme is derived for general elliptic interface problems with explicitly known functions of the solution and its normal flux at interface. Cao et al. [24] introduced and proved some superconvergence results for immersed finite volume methods(IFVM) for one dimensional interface problems with discontinuous diffusion coefficient and the connection conditions on interface being $[u] = 0$,$[\kappa\partial u/\partial\vec{n}] = 0$. Wang [25] presented IFVM for solving second-order elliptic problems with discontinuous d-iffusion coefficient on a Cartesian mesh. The recently developed immersed finite element (IFE) methods [28, 30, 35, 37, 38, 39, 40, 41, 42, 43, 44, 47, 52, 53, 56] employ an alternative idea to handle interface problems, such as the elasticity interface problems [42, 43, 53], the planar elasticity interface problems [44, 45], the parabolic equations with moving interface [28, 29], the Helmholtz equation [47], the elliptic interface inverse problems [38, 39], and three-dimensional second order elliptic interface problem [40, 41, 56]. He [27] analyzed the error in both the bilinear and linear IFE solutions for second-order elliptic boundary problems with discontinuous coefficients, the jump condition on interface are $[u] = 0$,$[\kappa\partial u/\partial\vec{n}] = 0$. In [28, 29] IFE methods for solving parabolic equations with discontinuous diffusion coefficientis across a time dependent interface are presented. He et al. [30] proposed a selective immersed discontinuous Galerkin method based on bilinear IFE for solving second-order elliptic interface problems. The selective feature of this method can be used to reduce the computational cost and/or incorporate desirable features in the numerical solver. Feng et al. [31] combined IFE and algebraic multigrid solver to solve the linear systems of the bilinear and linear IFE methods for both stationary and moving interface problems with discontinuous coefficient. Guo [32, 33] developed a nonconforming IFE method for second-order elliptic problems with discontinuous diffusion coefficient and $[u] = 0$, $[\kappa\partial u/\partial\vec{n}] = 0$. He et. al [34] developed IFE functions for solving second order elliptic boundary value problems with discontinuous coefficients and non-homogeneous jump conditions. Lin et al. [35] proposed IFE methods for solving boundary value problems of 4-th order differential equations with discontinuous coefficients and for sovling the interface problems of the Helmholtz equation [47] , where the interface jump conditions for the bi-harmonic equation are $[u]_\Gamma = 0$, $[\frac{\partial u}{\partial\vec{n}}]_\Gamma = 0$, $[\kappa(x, y)\triangle u(x, y)]_\Gamma = 0$, $[\frac{\partial\kappa(x,y)\triangle u(x,y)}{\partial\vec{n}}]_\Gamma = 0$. Guo [37] developed and analyzed a p-th degree IFE method for solving the elliptic interface problems with discontinuous coefficient. In [40, 41] an IFE method for solving the typical three-dimensional second order elliptic interface problem with discontinous coefficient are presented. Lin et. al [46] derived a priori error estimates for a class of interior penalty discontinuous Galerkin (DG) methods using IFE functions for a classic second-order elliptic interface problem. Adjerid et al. [55] presented and analyzed a p-th degree IFE method for elliptic interface problems with nonhomogeneous jump conditions, which is based on a discontinuous Galerkin formulation on interface elements and a continuous Galerkin formulation on non-interface elements and proved to converge optimally under mesh refinement. Han et al. [56] presented a three-dimensional (3D) linear IFE method with non-homogeneous flux jump conditions for solving electrostatic field involving complex boundary conditions using structured meshes independent of the interface. Lin et al. proposed partially penalized immersed finite element (PPIFE) method-s for elliptic interface problems [49] and parabolic interface problems [50]. Yang et al. [51] proved a approximation of second-order hyperbolic interface problems by partially penalized immersed finite element methods have optimal $O(h)$ convergence in an energy norm under a sub-optimal piecewise H^3 regularity assumption. Guo [52] proved the partially penalized immersed finite element (PPIFE) methods developed in [49, 50] converge optimally under the standard piecewise H^2 regularity assumption for the exact solution. Adjerid et al. [54] proved optimal a-priori error bounds for this PPIFE method not only in the energy norm but also in L_2 norm under the standard piecewise H^2 regularity assumption in the space variable of the exact solution. Guo et al. [38] presented a IFE method for solving a class of interface inverse problems for the typical elliptic interface problems and solving a group of inverse geometric problems for recovering the material interface of a linear elasticity system [39]. These interface inverse problems are formulated as shape optimization for recovering the interface which is reduced to a constrained optimization problem.

However, when the jumps are implicit along the interface problems, numerically solving the resulting problem becomes more challenging. The elliptic problems with imperfect contact are discussed in [1, 2, 3], where interface are aligned with grid points and the grid is orthogonal. A second order difference scheme for the elliptic problems with imperfect contact condition (2) is derived and studied in [57], where the condition that the flux κu_x is two-times continuously differentiable on the interface. Lin et al. [48] derived the error estimates for a class of IFE methods for elliptic interface problems with both perfect and imperfect interface jump conditions. It is worth pointing out that the coefficients of the scheme of linear element space in [48] is the same as those in this paper at regular points, but they are different at irregular points. The scheme of quadratic finite element and cubic finite element space is completely different from that in this paper. Cao et al. [58] presented a monotone finite volume scheme for the diffusion equation with imperfect interface which can obtain second order accuracy solution on the body fitted quadrilateral and triangular meshes. Zhou et al. [59] proposed a finite volume scheme preserving discrete maximum principle (DMP) for the diffusion equation with imperfect interface. Wang et al. [36] proposed a finite element method for solving parabolic interface problems with nonhomogeneous flux jump condition and nonlinear jump condition. Gwanghyun Jo et al. [12] enriched usual P_1-conforming finite element space and proposed a numerical methods for elliptic interface problems with implicit jump conditions, where the jumps are related to the normal fluxes and some known functions, i.e., $[u] = \alpha\frac{\partial u^+}{\partial \vec{n}^+} + h_1$, $[\beta\frac{\partial u}{\partial \vec{n}}] = h_2$.

The objective of the present paper is to introduce a finite difference method with second order for solving elliptic imperfect interface equations with implicit jump conditions. The original second-order immersed interface method of LeVeque and Li [15] focuses on the elliptic imperfect interface problems with explicit jump conditions. In this paper the elliptic equations with imperfect interface is considered, in which the jumps of physical quantities are unknown and proportional to the flux across the interface. This kind of interface connection condition has clear physical meaning. A finite difference method is constructed for the one dimensional elliptic equations with the imperfect contact and implicit jump conditions. The stability and convergence analysis are provided for the scheme. Numerical results show that the presented scheme has second order accuracy for linear elliptic imperfect interface problems with single or multiple interfaces.

The rest of this paper is organized as follows. In Section 2, we first formulate the scheme for 1D elliptic equations with imperfect interfaces. Sections 3 and 4 are devoted to analyze the stability and convergent rate of the scheme. Numerical examples are carried out in Section 5 to demonstrate the accuracy and stability of the presented scheme. A conclusion remark is given in Section 6.

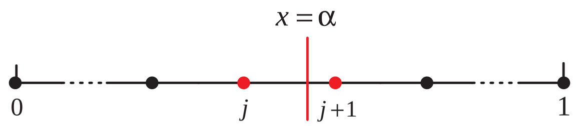

FIGURE 1. The stencil for 1D problem.

2. Construction of Difference Scheme

Consider the following elliptic boundary value problem

$$-(\beta(x)u_x)_x + k(x)u = f(x), \quad x \in (0,\alpha)\cup(\alpha,1), \tag{3}$$

$$u(0) = u_0, \quad u(1) = u_1, \tag{4}$$

where $0 < \alpha < 1$. And on the interface $x = \alpha$, consider the following imperfect contact condition

$$\begin{cases} [u] = \lambda\beta^+ u_x^+, \\ [\beta u_x] = 0, \end{cases} \tag{5}$$

where $g^\pm$ denote the right and left limits of the function g at the point α, and $[u] = u^+ - u^-$, $[\beta u_x] = \beta^+ u_x^+ - \beta^- u_x^-$.

We assume that $\beta(x)$ is piecewise smooth function with a jump at interface $x = \alpha$, and $\beta(x)$ is bounded from below and above

$$0 < \beta_{min} \le \beta(x) \le \beta_{max}, \tag{6}$$

where β_{min} and β_{max} are two constants. The function $k(x) \ge 0$, and the source term $f(x)$, are piecewise smooth.

By introducing the interface condition in the elliptic equation, we have

$$-(\beta(x)u_x)_x + k(x)u = f(x) + \frac{\beta^+ + \beta^-}{2}\lambda\beta(\alpha)u_x(\alpha)\delta'(x-\alpha), \quad x \in (0,1). \tag{7}$$

Introduce a uniform grid $x_i = ih, i = 0, 1, \cdots, n$ with $h = \frac{1}{n}$. The finite difference scheme can be written as

$$L_h u_h(x_i) = \gamma_{i,1}u_h(x_{i-1}) + \gamma_{i,2}u_h(x_i) + \gamma_{i,3}u_h(x_{i+1}) + k(x_i)u_h(x_i) = F_i, \tag{8}$$

for $i = 1, 2, \cdots, n-1$. Assume $x_j \le \alpha \le x_{j+1}$. The stencil is shown in Fig. 1.

At a regular point, i.e., $i \ne j, j+1$, L_h is the usual central difference approximation

$$\gamma_{i,1} = -\frac{\beta(x_{i-\frac{1}{2}})}{h^2}, \quad \gamma_{i,2} = -(\gamma_{i,1} + \gamma_{i,3}), \quad \gamma_{i,3} = -\frac{\beta(x_{i+\frac{1}{2}})}{h^2}, \tag{9}$$

and

$$F_i = f(x_i), \tag{10}$$

where $x_{i-\frac{1}{2}} = (x_i + x_{i-1})/2$ for $i = 1, 2, \cdots, n$.

The local truncation error is $O(h^2)$:

$$T_i = \gamma_{i,1}u(x_{i-1}) + \gamma_{i,2}u(x_i) + \gamma_{i,3}u(x_{i+1}) + k(x_i)u(x_i) - F_i = O(h^2), i \ne j, j+1. \tag{11}$$

At the irregular points x_j, x_{j+1}, the coefficients in (8) are determined as follows. Expand u_{j-1}, u_j, u_{j+1} in Taylor series about the point $x=\alpha$

$$u(x_{j-1}) = u^- + (x_{j-1}-\alpha)u_x^- + \frac{(x_{j-1}-\alpha)^2}{2}u_{xx}^- + O(h^3), \tag{12}$$

$$u(x_j) = u^- + (x_j-\alpha)u_x^- + \frac{(x_j-\alpha)^2}{2}u_{xx}^- + O(h^3), \tag{13}$$

$$u(x_{j+1}) = u^+ + (x_{j+1}-\alpha)u_x^+ + \frac{(x_{j+1}-\alpha)^2}{2}u_{xx}^+ + O(h^3), \tag{14}$$

Let $F_j = f^-(\alpha) + R_j$, and note that

$$k(x_j)u(x_j) = k^-(\alpha)u^-(\alpha) + O(h).$$

According to the interface connection condition (5), we have

$$u^+ = u^- + \lambda\beta^- u_x^-, \quad u_x^+ = \beta^- u_x^-/\beta^+.$$

Since

$$-\beta^+ u_{xx}^+ - \beta_x^+ u_x^+ + k^+u^+ - f^+ = -\beta^- u_{xx}^- - \beta_x^- u_x^- + k^-u^- - f^-,$$

it follows

$$u_{xx}^+ = \frac{1}{\beta^+}(\beta^- u_{xx}^- + (k^+\lambda\beta^- - \frac{\beta_x^+\beta^- - \beta_x^-\beta^+}{\beta^+})u_x^- + [k]u^- - [f]).$$

So

$$\begin{aligned} u(x_{j+1}) &= u^-(1+\frac{(x_{j+1}-\alpha)^2[k]}{2\beta^+}) + \frac{(x_{j+1}-\alpha)^2\beta^-}{2\beta^+}u_{xx}^- - \frac{(x_{j+1}-\alpha)^2}{2\beta^+}[f] \\ &+ \left(\lambda\beta^- + \frac{\beta^-}{\beta^+}(x_{j+1}-\alpha) + (\frac{k^+\lambda\beta^-}{\beta^+} - \frac{\beta_x^+\beta^- - \beta_x^-\beta^+}{{\beta^+}^2})\frac{(x_{j+1}-\alpha)^2}{2}\right)u_x^-. \end{aligned} \tag{15}$$

Then

$$\begin{aligned} T_j &= \gamma_{j,1}u(x_{j-1}) + \gamma_{j,2}u(x_j) + \gamma_{j,3}u(x_{j+1}) + k(x_j)u(x_j) - F_j \\ &= \gamma_{j,1}u(x_{j-1}) + \gamma_{j,2}u(x_j) + \gamma_{j,3}u(x_{j+1}) + k^-(\alpha)u^-(\alpha) \\ &\quad -(-\beta^- u_{xx}^- - \beta_x^- u_x^- + k^-u^-) - R_j + O(h). \end{aligned} \tag{16}$$

Substituting (13),(14) and (15) into the above equation (16) and rearranging, there is

$$\begin{aligned} T_j &= \left(\gamma_{j,1} + \gamma_{j,2} + \gamma_{j,3}(1+\frac{(x_{j+1}-\alpha)^2[k]}{2\beta^+})\right)u^- + \Bigg\{(x_{j-1}-\alpha)\gamma_{j,1} + (x_j-\alpha)\gamma_{j,2} \\ &+ \left(\lambda\beta^- + \frac{\beta^-}{\beta^+}(x_{j+1}-\alpha) + (\frac{k^+\lambda\beta^-}{\beta^+} - \frac{\beta_x^+\beta^- - \beta_x^-\beta^+}{{\beta^+}^2})\frac{(x_{j+1}-\alpha)^2}{2}\right)\gamma_{j,3} + \beta_x^-\Bigg\}u_x^- \\ &+ \frac{1}{2}\left\{(x_{j-1}-\alpha)^2\gamma_{j,1} + (x_j-\alpha)^2\gamma_{j,2} + (x_{j+1}-\alpha)^2\frac{\beta^-}{\beta^+}\gamma_{j,3} + 2\beta^-\right\}u_{xx}^- \\ &- \gamma_{j,3}\frac{(x_{j+1}-\alpha)^2[f]}{2\beta^+} - R_j + O(h). \end{aligned}$$

Require $\gamma' s$ and R_j to satisfy

$$(17)\quad \begin{cases} \gamma_{j,1}+\gamma_{j,2}+\gamma_{j,3}(1+\frac{(x_{j+1}-\alpha)^2[k]}{2\beta^+})=0, \\ \gamma_{j,1}(x_{j-1}-\alpha)+\gamma_{j,2}(x_j-\alpha)+\gamma_{j,3}\Big\{\lambda\beta^-+\frac{\beta^-}{\beta^+}(x_{j+1}-\alpha) \\ \qquad +(\frac{\lambda k^+\beta^-}{\beta^+}-\frac{\beta^-\beta_x^+-\beta_x^-\beta^+}{{\beta^+}^2})\frac{(x_{j+1}-\alpha)^2}{2}\Big\}=-\beta_x^-, \\ \gamma_{j,1}(x_{j-1}-\alpha)^2+\gamma_{j,2}(x_j-\alpha)^2+\gamma_{j,3}(x_{j+1}-\alpha)^2\frac{\beta^-}{\beta^+}=-2\beta^-, \end{cases}$$

and

$$R_j=-\gamma_{j,3}\frac{(x_{j+1}-\alpha)^2[f]}{2\beta^+}.$$

Similarly, the coefficients of the scheme at x_{j+1} are determined by the following system

$$(18)\quad \begin{cases} \gamma_{j+1,1}(1-\frac{(x_j-\alpha)^2[k]}{2\beta^-})+\gamma_{j+1,2}+\gamma_{j+1,3}=0, \\ \gamma_{j+1,1}\Big\{-\lambda\beta^++\frac{\beta^+}{\beta^-}(x_j-\alpha)-(\frac{\beta_x^-\beta^+-\beta_x^+\beta^-}{{\beta^-}^2}+\frac{\lambda\kappa^-\beta^+}{\beta^-})\frac{(x_j-\alpha)^2}{2}\Big\} \\ \qquad +\gamma_{j+1,2}(x_{j+1}-\alpha)+\gamma_{j+1,3}(x_{j+2}-\alpha)=-\beta_x^+, \\ \gamma_{j+1,1}(x_j-\alpha)^2\frac{\beta^+}{\beta^-}+\gamma_{j+1,2}(x_{j+1}-\alpha)^2+\gamma_{j+1,3}(x_{j+2}-\alpha)^2=-2\beta^+, \end{cases}$$

and

$$R_{j+1}=\gamma_{j+1,1}\frac{(x_j-\alpha)^2[f]}{2\beta^-}.$$

If $\beta_x^+=\beta_x^-=0$ and $k(x)$ is continuous for $x\in(0,\alpha)\cup(\alpha,1)$, then

$$\begin{cases} \gamma_{j,1}=\frac{\frac{\beta^-}{\beta^+}(-2\lambda\beta^+\beta^--2\beta^-(x_{j+1}-\alpha)-\lambda\kappa(\alpha)\beta^-(x_{j+1}-\alpha)^2+2\beta^+(x_j-\alpha))}{D_j}, \\ \gamma_{j,2}=\frac{-\frac{\beta^-}{\beta^+}(-2\lambda\beta^+\beta^--2\beta^-(x_{j+1}-\alpha)-\lambda\kappa(\alpha)\beta^-(x_{j+1}-\alpha)^2+2\beta^+(x_{j-1}-\alpha))}{D_j}, \\ \gamma_{j,3}=\frac{-2\beta^-h}{D_j}, \end{cases}$$

where

$$\begin{aligned} D_j &= \frac{h}{\beta^+}\Big\{-\big(\lambda\beta^+\beta^-+\lambda\kappa(\alpha)\beta^-\frac{(x_{j+1}-\alpha)^2}{2}\big)(x_{j-1}+x_j-2\alpha) \\ &+ 2\beta^-h^2+[\beta](x_{j-1}-\alpha)(x_j-\alpha)\Big\}. \end{aligned}$$

And

$$\begin{cases} \gamma_{j+1,1}=\frac{-2\beta^+h}{D_{j+1}}, \\ \gamma_{j+1,2}=\frac{\frac{\beta^+}{\beta^-}(2\lambda\beta^+\beta^-+2\beta^-(x_{j+2}-\alpha)+\lambda\kappa(\alpha)\beta^+(x_j-\alpha)^2-2\beta^+(x_j-\alpha))}{D_{j+1}}, \\ \gamma_{j+1,3}=\frac{-\frac{\beta^+}{\beta^-}(\lambda\beta^+\beta^-+2\beta^-(x_{j+1}-\alpha)+\lambda\kappa(\alpha)\beta^+(x_j-\alpha)^2-2\beta^+(x_j-\alpha))}{D_{j+1}}, \end{cases}$$

where

$$\begin{aligned} D_{j+1} &= \frac{h}{\beta^-}\Big\{\big(\lambda\beta^+\beta^-+\lambda\kappa(\alpha)\beta^+\frac{(x_j-\alpha)^2}{2}\big)(x_{j+1}+x_{j+2}-2\alpha) \\ &- 2\beta^+h^2-[\beta](x_{j+1}-\alpha)(x_{j+2}-\alpha)\Big\}. \end{aligned}$$

3. Stability

From the expression obtained above, we can get the following lemma.

Lemma 1 Assume $\beta_x^+ = \beta_x^- = 0$ and $k(x) \equiv 0$ for $x \in (0, \alpha) \cup (\alpha, 1)$. Then for h small

(1) there are positive constants C_1 and C_2 such that

$$\frac{C_1}{h} \le |\gamma_{j,3}| \le \frac{C_2}{h}, \quad \frac{C_1}{h} \le |\gamma_{j+1,1}| \le \frac{C_2}{h},$$

and for all other $\gamma' s$

$$\frac{C_1}{h^2} \le |\gamma_{i,k}| \le \frac{C_2}{h^2};$$

(2) the conditions of the maximum principle are satisfied, that is

$$\gamma_{i,1} < 0, \gamma_{i,3} < 0, \gamma_{i,2} > 0, \quad and \quad |\gamma_{i,1}| + |\gamma_{i,3}| \le \gamma_{i,2}.$$

Remark In the case of $\beta_x^{\pm} \neq 0$ and $[k] \neq 0$, the conclusion of lemma still holds except replacing the inequality in (2) by

$$|\gamma_{i,1}| + |\gamma_{i,3}| \le \gamma_{i,2} - k(x_i).$$

The following lemma can be found in [19] and [60].

Lemma 2 For a difference scheme L_h defined on a discrete set of interior points J_Ω, we assume

(1) J_Ω is partitioned into a number of disjoint regions

$$J_\Omega = J_1 \cup J_2 \cup \cdots \cup J_s, \quad J_i \cap J_k = \emptyset, \quad for \quad i \neq k;$$

(2) The truncation error of the difference scheme at a grid point p satisfies

$$|T_p| \le T_i, \quad \forall p \in J_i, \quad i = 1, 2, \cdots, s;$$

(3) There exists a non-negative mesh function ϕ defined on $\cup_{i=1}^s J_i$ satisfying

$$L_h \phi_p \ge C_i > 0, \quad \forall p \in J_i, \quad i = 1, 2, \cdots, s;$$

Then

$$\|E_h\|_\infty \le \left(\max_{A \in J_{\partial\Omega}} \phi_A \right) \max_{1 \le i \le s} \left\{ \frac{T_i}{C_i} \right\},$$

where $E_h(x_i) = u(x_i) - u_h(x_i)$ and $J_{\partial\Omega}$ is the set of boundary points.

The usual stability result can be obtained by letting $C_i = 1$ for $i = 1, 2, \cdots$, and

$$\phi_p = \frac{\beta^-}{2}(x-\alpha)^2, \quad x < \alpha; \quad \phi_p = \frac{\beta^+}{2}(x-\alpha)^2, \quad x > \alpha;$$

The convergence rate of at least first-order follows immediately from $T_i = O(h)$.

4. Convergent analysis

4.1. Comparison Function. Consider the special case of $\beta_x^+ = \beta_x^- = 0$ and $k(x) \equiv 0$.

Let

$$\phi(x) = \begin{cases} \frac{(x-\alpha)^2}{2\beta^-} + \xi_1(\alpha - x) + \xi_2(x_j - x), & for \quad x \le \alpha, \\ \frac{(x-\alpha)^2}{2\beta^+} + \xi_3(\alpha - x) + \xi_4(x - x_{j+1}), & for \quad x > \alpha. \end{cases}$$

Here $\xi_k (k = 1, 2, 3, 4)$ are positive constants satisfying $\xi_1 + \xi_2 \ge \frac{4}{\beta^-}$, $\xi_3 + \xi_4 \ge \frac{4}{\beta^+}$. Direct calculation gives

$$L_h \phi_i = 1, \quad i = 1, 2, \cdots, j-1, j+2, \cdots, n-1,$$

$$L_h\phi_j > \frac{1}{h}, \quad L_h\phi_{j+1} > \frac{1}{h}, \quad \text{when } h \text{ is small enough.}$$

The local truncation error of the difference scheme (8) constructed in section 1 is bounded by

$$|T_i| \le \frac{\beta_{max}M_{xxxx}}{12}h^2, \quad i = 1, 2, \cdots, j-1, j+2, \cdots, n-1,$$

$$|T_j| \le \frac{3\gamma_{max}M_{xxx}}{2}h, \quad |T_{j+1}| \le \frac{3\gamma_{max}M_{xxx}}{2}h,$$

where

$$\gamma_{max} = \max_{1\le j\le n-1}\max_{1\le k\le 3}|\gamma_{j,k}|h^2,$$

$$M_{xxx} = max\Big\{\max_{x<\alpha}|u^{'''}(x)|, \max_{x>\alpha}|u^{'''}(x)|\Big\},$$

$$M_{xxxx} = max\Big\{\max_{x<\alpha}|u^{''''}(x)|, \max_{x>\alpha}|u^{''''}(x)|\Big\}.$$

By using the Lemma 2 we obtain the following convergence result.

Theorem 3 Under the same condition as lemma 1, there holds

$$\|u(x_i) - u_h(x_i)\|_\infty \le \frac{3}{2}\gamma_{max}M\phi_{max}h^2,$$

where

$$\phi_{max} = max(\phi(0), \phi(1)), \quad M = max(M_{xxx}, M_{xxxx}).$$

4.2. Asymptotic Error Expansion. Lemma 4 There exists a piecewise smooth function $\hat{U}$ satisfying $\hat{U}(0) = u_0, \hat{U}(1) = u_1$ and

$$L_h\hat{U}(x_i) - F_i = O(h^2), \quad i = 1, 2, \cdots, n-1,$$

moreover, it is an order $O(h^2)$ perturbation of u

$$\hat{U} = u + \sum_{p=2}^{q-1} h^p u^{(p)},$$

where $u^{(p)}$ and their derivatives depend on u and its derivatives, provided that $q \ge 4$ and the original solution u is sufficiently smooth in each sub-domain.

Proof Without loss of generality, we assume $[k] = 0$ and $[f] = 0$. For $i \ne j, j+1$, $\hat{U}$ is smooth. Note that

$$\begin{aligned} L_h\hat{U}(x_i) - F_i &= \gamma_{i,1}\hat{U}(x_{i-1}) + \gamma_{i,2}\hat{U}(x_i) + \gamma_{i,3}\hat{U}(x_{i+1}) + k(x_i)\hat{U}(x_i) - f(x_i) \\ &= (\gamma_{i,1} + \gamma_{i,2} + \gamma_{i,3})\hat{U}(x_i) + h(-\gamma_{i,1} + \gamma_{i,3})\hat{U}_x(x_i) \\ &+ \frac{h^2}{2}(\gamma_{i,1} + \gamma_{i,3})\hat{U}_{xx}(x_i) + \frac{h^2}{6}(-\gamma_{i,1} + \gamma_{i,3})\hat{U}_{xxx}(x_i) \\ &+ k(x_i)\hat{U}(x_i) - f(x_i) + O(h^4\gamma). \end{aligned}$$

Substituting $\hat{U} = \sum_{p=0}^{q-1} h^p u^{(p)}$ into above equality and picking up the terms in the same order of h gives

$$\begin{aligned} h^0 &: (\beta u_x^{(0)})_x + ku^{(0)} - f = 0; \\ h^1 &: (\beta u_x^{(1)})_x + ku^{(1)} = 0; \\ h^2 &: (\beta u_x^{(2)})_x + ku^{(2)} = -\frac{1}{12}u_{xxxx}^{(0)}. \end{aligned}$$

At the boundary points $x = 0$ and $x = 1$, by requiring $\hat{U}(x_0) = u(x_0)$ and $\hat{U}(x_n) = u(x_n)$, we get

$$\begin{aligned} h^0 &\ : \ u^{(0)}(x_0) = u(x_0), \quad u^{(0)}(x_n) = u(x_n); \\ h^1 &\ : \ u^{(1)}(x_0) = 0, \quad u^{(1)}(x_n) = 0; \\ h^2 &\ : \ u^{(2)}(x_0) = 0, \quad u^{(2)}(x_n) = 0. \end{aligned}$$

For $i = j$, we hope $L_h\hat{U}(x_j) - F_j = O(h^2)$. There holds

$$\begin{aligned} L_h\hat{U}(x_j) - F_j &= \gamma_{j,1}\hat{U}(x_{j-1}) + \gamma_{j,2}\hat{U}(x_j) + \gamma_{j,3}\hat{U}(x_{j+1}) + k(\alpha)\hat{U}(\alpha^-) - f(\alpha) \\ &= (\gamma_{j,1} + \gamma_{j,2} + \gamma_{j,3})\hat{U}(\alpha^-) \\ &+ \left((x_{j-1} - \alpha)\gamma_{j,1} + (x_j - \alpha)\gamma_{j,2} + \frac{\beta^-(x_{j+1} - \alpha)}{\beta^+}\gamma_{j,3}\right)\hat{U}_x(\alpha^-) \\ &+ \frac{1}{2}\left((x_{j-1} - \alpha)^2\gamma_{j,1} + (x_j - \alpha)^2\gamma_{j,2} + (x_{j+1} - \alpha)^2\frac{\beta^-}{\beta^+}\gamma_{j,3}\right)\hat{U}_{xx}(\alpha^-) \\ &+ \frac{1}{6}\left((x_{j-1} - \alpha)^3\gamma_{j,1} + (x_j - \alpha)^3\gamma_{j,2} + (x_{j+1} - \alpha)^3\frac{\beta^-}{\beta^+}\gamma_{j,3}\right)\hat{U}_{xxx}(\alpha^-) \\ &+ \gamma_{j,3}[\hat{U}] + (x_{j+1} - \alpha)\gamma_{j,3}\frac{[\beta\hat{U}_x]}{\beta^+} + (x_{j+1} - \alpha)^2\gamma_{j,3}\frac{[\beta\hat{U}_{xx}]}{2\beta^+} \\ &+ (x_{j+1} - \alpha)^3\gamma_{j,3}\frac{[\beta\hat{U}_{xxx}]}{6\beta^+} + k(\alpha)\hat{U}(\alpha^-) - f(\alpha) + O(h^4\gamma). \end{aligned}$$

From (17) it follows

$$\begin{aligned} L_h\hat{U}(x_j) - F_j &= \gamma_{j,3}([\hat{U}] - \lambda\beta^-\hat{U}_x(\alpha^-)) + (x_{j+1} - \alpha)\gamma_{j,3}\frac{[\beta\hat{U}_x]}{\beta^+} \\ &+ (x_{j+1} - \alpha)^2\gamma_{j,3}\frac{1}{2\beta^+}\left([\beta\hat{U}_{xx}] - \left(\beta_x^- - \frac{\beta^-\beta_x^+}{\beta^+} - \lambda k\beta^-\right)\hat{U}_x(\alpha^-)\right) \\ &+ \beta_x^-\hat{U}_x(\alpha^-) + \beta^-\hat{U}_{xx}(\alpha^-) + k(\alpha)\hat{U}(\alpha^-) - f(\alpha) \\ &+ \frac{1}{6}\left((x_{j-1} - \alpha)^3\gamma_{j,1} + (x_j - \alpha)^3\gamma_{j,2} + (x_{j+1} - \alpha)^3\gamma_{j,3}\frac{\beta^-}{\beta^+}\right)\hat{U}_{xxx}(\alpha^-) \\ &+ (x_{j+1} - \alpha)^3\gamma_{j,3}\frac{1}{6\beta^+}[\beta\hat{U}_{xxx}] + O(h^4\gamma). \end{aligned}$$

Substituting $\hat{U} = \sum_{p=0}^{q-1} h^p u^{(p)}$ into above equality and picking up the terms in the same order of h we get

$$\begin{aligned} h^0 &\ : \ \gamma_{j,3}([u^{(0)}] - \lambda\beta^- u_x^{(0)}(\alpha^-)) = 0; \\ h^1 &\ : \ \gamma_{j,3}h([u^{(1)}] - \lambda\beta^- u_x^{(1)}(\alpha^-)) + (x_{j+1} - \alpha)\gamma_{j,3}\frac{[\beta u_x^{(0)}]}{\beta^+} = 0; \\ h^2 &\ : \ \gamma_{j,3}h^2([u^{(2)}] - \lambda\beta^- u_x^{(2)}(\alpha^-)) + (x_{j+1} - \alpha)\gamma_{j,3}\frac{h[\beta u_x^{(1)}]}{\beta^+} \\ &\quad + (x_{j+1} - \alpha)^2\gamma_{j,3}\frac{1}{2\beta^+}\left\{[\beta u_{xx}^{(0)}] - \left(\beta_x^- - \frac{\beta^-\beta_x^+}{\beta^+} - \lambda\kappa\beta^-\right)u_x^{(0)}(\alpha^-)\right\} \\ &\quad + \frac{1}{6}((x_{j-1} - \alpha)^3\gamma_{j,1} + (x_j - \alpha)^3\gamma_{j,2})\hat{U}_{xxx}(\alpha^-) = 0; \end{aligned}$$

$$
\begin{aligned}
h^3 \quad : \quad & \gamma_{j,3}h^3([u^{(3)}] - \lambda\beta^- u_x^{(3)}(\alpha^-) + (x_{j+1}-\alpha)\gamma_{j,3}\frac{h^2}{\beta^+}[\beta u_x^{(2)}] \\
& +(x_{j+1}-\alpha)^2\gamma_{j,3}\frac{h}{2\beta^+}\Big\{[\beta u_{xx}^{(1)}] - (\beta_x^- - \frac{\beta^-\beta_x^+}{\beta^+} - \lambda\kappa\beta^-)u_x^{(1)}(\alpha^-)\Big\} \\
& +(x_{j+1}-\alpha)^3\gamma_{j,3}\frac{\beta^-}{6\beta^+}u_{xxx}^{(0)}(\alpha^-) + (x_{j+1}-\alpha)^3\gamma_{j,3}\frac{1}{6\beta^+}[\beta u_{xxx}^{(0)}] \\
& +\frac{1}{6}((x_{j-1}-\alpha)^3\gamma_{j,1} + (x_j-\alpha)^3\gamma_{j,2})hu_{xxx}^{(1)}(\alpha^-) = 0.
\end{aligned}
$$

Similarly for $i = j+1$ we can obtain

$$
\begin{aligned}
h^0 \quad : \quad & \gamma_{j+1,1}([u^{(0)}] - \lambda\beta^+ u_x^{(0)}(\alpha^+) = 0; \\
h^1 \quad : \quad & \gamma_{j+1,1}h([u^{(1)}] - \lambda\beta^+ u_x^{(1)}(\alpha^+)) + (x_j-\alpha)\gamma_{j+1,1}\frac{1}{\beta^-}[\beta u_x^{(0)}] = 0; \\
h^2 \quad : \quad & \gamma_{j+1,1}h^2([u^{(2)}] - \lambda\beta^+ u_x^{(2)}(\alpha^+)) + (x_j-\alpha)\gamma_{j,3}\frac{h}{\beta^-}[\beta u_x^{(1)}] \\
& +(x_j-\alpha)^2\gamma_{j+1,1}\frac{1}{2\beta^-}\Big\{[\beta u_{xx}^{(0)}] + (\beta_x^+ - \frac{\beta_x^-\beta^+}{\beta^-} - \lambda\kappa\beta^+)u_x^{(0)}(\alpha^+)\Big\} \\
& -\frac{1}{6}((x_{j+1}-\alpha)^3\gamma_{j+1,2} + (x_{j+2}-\alpha)^3\gamma_{j+1,3})\hat{U}_{xxx}(\alpha^+) = 0; \\
h^3 \quad : \quad & -\gamma_{j+1,1}h^3([u^{(3)}] - \lambda\beta^+ u_x^{(3)}(\alpha^+) - (x_j-\alpha)\gamma_{j+1,1}\frac{h^2}{\beta^-}[\beta u_x^{(2)}] \\
& -(x_j-\alpha)^2\gamma_{j+1,1}\frac{h}{2\beta^-}\Big\{[\beta u_{xx}^{(1)}] + (\beta_x^+ - \frac{\beta_x^-\beta^+}{\beta^-} - \lambda\kappa\beta^+)u_x^{(1)}(\alpha^-)\Big\} \\
& +\frac{1}{6}((x_{j+1}-\alpha)^3\gamma_{j+1,2} + (x_{j+2}-\alpha)^3\gamma_{j+1,3})u_{xxx}^{(1)}(\alpha^+) \\
& +(x_j-\alpha)^3\gamma_{j+1,1}\frac{1}{6}\frac{\beta^+}{\beta^-}u_{xxx}^{(0)}(\alpha^+) - (x_j-\alpha)^3\gamma_{j+1,1}\frac{1}{6}\frac{[\beta u_{xxx}^{(0)}]}{\beta^-} = 0.
\end{aligned}
$$

From the above equations it follows

$$
\begin{aligned}
[u^{(0)}] = \lambda\beta^+ u_x^{(0)}(\alpha^-), \quad [\beta u_x^{(0)}] = 0, \\
[u^{(1)}] = \lambda\beta^+ u_x^{(1)}(\alpha^-), \quad [\beta u_x^{(1)}] = 0.
\end{aligned}
$$

From the uniqueness of the solution to (3) - (5), we get

$$u^{(0)} \equiv u, \quad u^{(1)} \equiv 0.$$

Also the jump condition for $u^{(2)}$ can be derived. Then the equations with boundary and interface conditions can be solved, and the solutions are piecewise smooth and bounded. So $\hat{U} = u + O(h^2)$. The proof of the lemma is completed.

Denote $\hat{E}_h = \hat{U} - u_h$. By applying the Lemma 2 for $\hat{E}_h$ we obtain

Lemma 5 Under the same conditions of Lemma 2, there holds

$$\|\hat{E}_h\|_\infty \le Ch^2,$$

where C is a constant.

Finally the following error estimate is derived.

Theorem 6 Let u be the solutions of (3)-(5) and u_h be the solution of difference scheme (8) constructed in section 2. Then

$$\|u(x_i) - u_h(x_i)\|_\infty \le Ch^2,$$

TABLE 1. The L_2 and L_∞ errors for Example 1, $k = 100$.

Mesh \ Error	L_2^u	rate	L_∞^u	rate
128	7.58e-3		1.74e-2	
256	3.82e-3	1.01	9.19e-3	0.95
512	9.44e-4	2.03	2.27e-3	2.01
1204	2.31e-4	2.01	5.56e-4	2.03
2048	5.54e-5	2.04	1.33e-4	2.06

TABLE 2. The L_2 and L_∞ errors for Example 1, $k = 1000$.

Mesh \ Error	L_2^u	rate	L_∞^u	rate
128	7.57e-2		1.74e-1	
256	3.82e-2	0.98	9.19e-2	0.92
512	9.44e-3	2.01	2.27e-2	2.01
1204	2.31e-3	2.03	5.56e-3	2.03
2048	5.54e-4	2.06	1.33e-3	2.06

where $C = \|u^{(2)}\|_\infty + O(1)$.

Proof Obviously, by Lemmas 3 and 4

$$\begin{aligned}\|u(x_i) \quad - \quad u_h(x_i)\|_\infty &\le \|u(x_i) - \hat{U}_h(x_i)\|_\infty + \|\hat{U}(x_i) - u_h(x_i)\|_\infty \\ &\le \quad \|\sum_{2}^{q-1} h^p u^{(p)}\|_\infty + O(h^2) \le (\|u^{(2)}\|_\infty + O(1))h^2.\end{aligned}$$

5. Numerical experiments

In this section, we use several numerical experiments to demonstrate the performance of the discrete schemes.

Example 1 Consider the computational domain $\Omega = [0, 1]$, and the solution is separated into two parts by the interface at $x = \alpha$, $\alpha = 0.543$. The analytical solution of this problem is given by

$$u(x, y) = \begin{cases} x^2, & x \in (0, \alpha), \\ \kappa e^{x^2}, & x \in (\alpha, 1), \end{cases}$$

The diffusion coefficient is defined as follows

$$\beta = \begin{cases} \kappa e^{x^2}, & x \in (0, \alpha), \\ 1, & x \in (\alpha, 1), \end{cases}$$

The conservation of the flux on interface is satisfied

$$[\beta \frac{\partial u}{\partial x}] = \beta^+ \frac{\partial u^+}{\partial x} - \beta^- \frac{\partial u^-}{\partial x} = 2\kappa x e^{x^2} - 2\kappa x e^{x^2} = 0, \quad at \quad x = \alpha.$$

The coefficient λ is given as

$$\lambda = \frac{\kappa e^{\alpha^2} - \alpha^2}{2\kappa\alpha e^{\alpha^2}}.$$

Tables 1 and 2 show the L_2 and L_∞ norms and convergent rate of unknowns at the ratio of diffusion coefficient being $k = 100$ and $k = 1000$, respectively. From

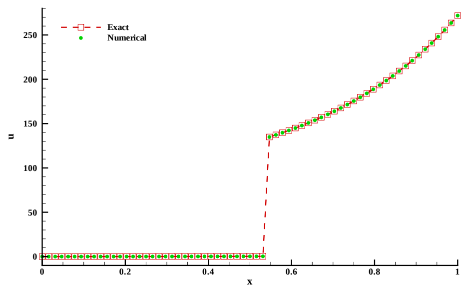

FIGURE 2. The comparison of exact and numerical solutions for Problem 1.

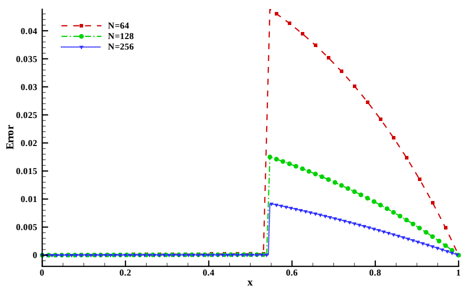

FIGURE 3. The comparison of errors at different mesh numbers for Problem 1).

these tables, we can see that this method obtains the second order convergent rate in L_2 and L_∞ norms of unknowns. It can be concluded that as the ratio of diffusion coefficient on both side of interface is increase, the convergent rate of unknowns and discrete flux remains almost same.

Fig. 2 displays the comparison of the numerical solution and exact solution at $k = 100$ on the mesh with the number of intervals is 32. It is shown that the numerical solutions are well matched with the exact solutions, in spite of the amount of physical jumps on both sides of the interface is much larger. Fig. 3 compares the errors under different mesh size. It can be seen that the errors are decreasing as the number of mesh point is increasing.

Example 2 Consider the linear problem which solution is separated into three parts by two interfaces at $\alpha_1 = 0.3$ and $\alpha_2 = 0.7$, respectively. The analytical solution of this problem is given by

$$u(x,y) = \begin{cases} \kappa e^{x^2}, & x \in (0, \alpha_1), \\ x^2, & x \in (\alpha_1, \alpha_2), \\ \kappa e^{x^2}, & x \in (\alpha_2, 1), \end{cases}$$

The diffusion coefficient is defined as follows

$$\beta = \begin{cases} 1, & x \in (0, \alpha_1), \\ \kappa e^{x^2}, & x \in (\alpha_1, \alpha_2), \\ 1, & x \in (\alpha_2, 1), \end{cases}$$

Then, the flux on interface is conservative and satisfied the connective condition on each interface $[\beta \frac{\partial u}{\partial x}]|_{x=\alpha_i} = 0, i = 1, 2.$

TABLE 3. The L_2 and L_∞ errors for Example 1, $k = 100$.

Mesh \ Error	L_2^u	rate	L_∞^u	rate
128	7.58e-3		1.74e-2	
256	3.82e-3	1.01	9.19e-3	0.95
512	9.44e-4	2.03	2.27e-3	2.01
1204	2.31e-4	2.01	5.56e-4	2.03
2048	5.54e-5	2.04	1.33e-4	2.06

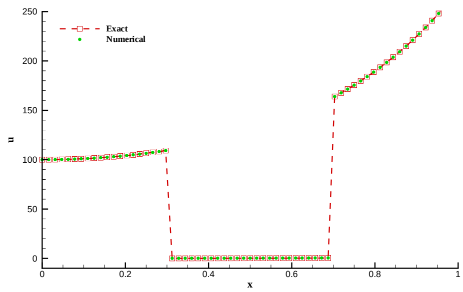

FIGURE 4. The comparison of exact and numerical solutions at $\kappa = 100$ with different mesh numbers for example 2.

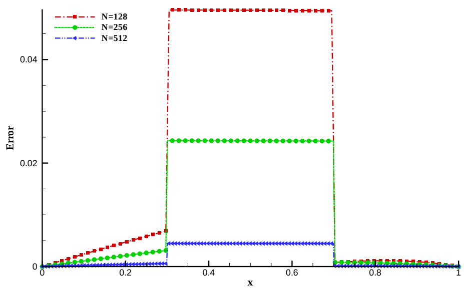

FIGURE 5. The comparison of errors at different mesh numbers for example 2.

Table 3 displays the L_2 and L_∞ norms and convergent rate of unknowns at the ratio of diffusion coefficient being $k = 100$. It can be seen that the numerical solution achieves second order convergent rate in L_2 and L_∞ norms.

Fig. 4 displays the comparison of the numerical solution and exact solution at $k = 100$ on the mesh with the number of intervals is 64. It is shown that the presented method is able to capture the discontinuities of the solution and efficiently fit with the exact solution. Fig. 5 compares the errors under different mesh size.

Example 3 Further, in order to test the efficiency of the presented numerical method the linear problem with four interfaces is considered. Location of four interfaces are $\alpha_1 = 0.1$, $\alpha_2 = 0.4$, $\alpha_3 = 0.6$, and $\alpha_4 = 0.9$, respectively. The

TABLE 4. The L_2 and L_∞ errors for Example 3, $\kappa = 10$.

Mesh \ Error	L_2^u	rate	L_∞^u	rate
64	5.54e-2		8.44e-2	
128	1.48e-2	1.90	2.15e-2	1.97
256	3.63e-3	2.02	4.99e-3	2.10
512	8.99e-4	2.01	1.36e-3	1.87
1024	2.37e-4	1.93	2.85e-4	2.02

TABLE 5. The L_2 and L_∞ errors for Example 3, $\kappa = 100$.

Mesh \ Error	L_2^u	rate	L_∞^u	rate
128	1.07e-1		1.74e-1	
256	1.84e-2	2.53	4.91e-2	1.82
512	4.41e-3	2.06	1.45e-2	1.76
1024	1.01e-3	2.12	2.65e-3	2.45
2048	2.44e-4	2.04	6.86e-4	1.95

analytical solution of this problem is given by

$$u(x,y) = \begin{cases} e^{x^2}, & x \in (0, \alpha_1), \\ \kappa e^{x^2}, & x \in (\alpha_1, \alpha_2), \\ x^2, & x \in (\alpha_2, \alpha_3), \\ \kappa e^{x^2}, & x \in (\alpha_3, \alpha_4), \\ e^{x^2}, & x \in (\alpha_4, 1), \end{cases}$$

The diffusion coefficient is defined as follows

$$\beta = \begin{cases} \kappa, & x \in (0, \alpha_1), \\ 1, & x \in (\alpha_1, \alpha_2), \\ \kappa e^{x^2}, & x \in (\alpha_2, \alpha_3), \\ 1, & x \in (\alpha_3, \alpha_4), \\ \kappa, & x \in (\alpha_4, 1). \end{cases}$$

Then, the flux on interface is conservative and satisfied the connective condition on each interface $[\beta\frac{\partial u}{\partial x}]|_{x=\alpha_i} = 0, i = 1, 2, 3, 4$.

From Tables 4 and 5, we can see that the presented scheme is able to obtain almost second order convergent rate in L_2 and L_∞ norms, even when there are four interfaces and the ratio of diffusion coefficient varies from 10 to 100.

Fig. 4 compares the numerical solution and exact solution for example 3 at $N = 64$ and $\kappa = 100$. It is shown that the presented scheme is strong enough to capture the jump condition on the solution and fit well with the exact solution. The L_2 norm errors under different mesh size are displayed in Fig. 7.

6. Conclusion

A finite difference scheme for elliptic equations with imperfect contact and implicit jump conditions is presented. The key feature of the implicit connection condition is that the jump qualities of the solution is unknown and related with the flux across the interface. The second-order difference schemes are constructed for

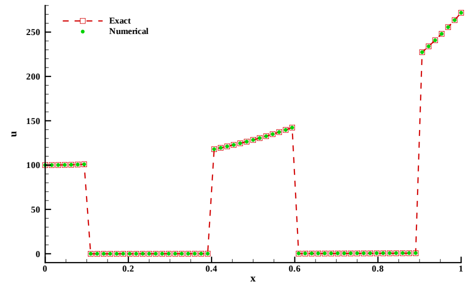

FIGURE 6. The comparison of exact and numerical solutions for example 3, at $N = 64$ and $\kappa = 100$.

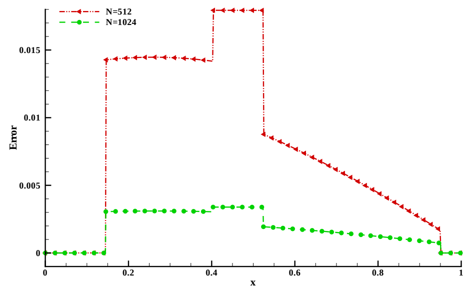

FIGURE 7. The comparison of errors at different mesh numbers for example 3, $\kappa = 100$.

one-dimensional elliptic interface problems. The stability and convergence property is analyzed for the schemes. Numerical results show that the presented scheme achieves second-order accuracy for the elliptic interface problems with implicit jump conditions for both single and multiple interfaces.

Acknowledgments

This work is partially supported by the National Natural Science Foundation of China (12161067,11571048,11971069, 51961031),the National Natural Science Youth Fund Project(11801287), inner Mongolia Autonomous Region "Youth Science and technology talents" support program (NJYT20B15), the Inner Mongolia Scientific Fund Project (NJZZ18140, 2018BS01002, 2018MS06002, 2018LH01008, 2019BS01007,2020MS06010, 2021LHMS01006), Innovation fund project of Inner Mongolia University of science and technology-Excellent Youth Science Fund Project(2019YQL02).

References

[1] Samarskii, A., Andreev,V.B., Differential method for elliptic equations[in Russian]. Nauka, Moscow, 1976.
[2] Samarskii, A., Theroy of difference scheme, Moscow, Nauka, 1977.
[3] Samarskii, A., Vabishchevich, P. N., Computational heat transfer, Vol. 1, John Wiley& Sons Ltd, 1995.
[4] Huang, Z., Ding, E., Transport theory (Second Edition), Science Press, Beijing, 2008.
[5] López-Ruiz, G., Bravo-Castillero,J., Brenner,R., et al. Variational bounds in composites with nonuniform interfacial thermal resistance, Appl. Math. Model., 2015, 39(23): 7266-7276.

[6] Matt, C., Cruz, M., Application of a multiscale finite-element approach to calculate the effective conductivity of particulate media, Comput. Appl. Math., 2002, 21(2): 429-460.
[7] Rocha, R., Cruz, M., Computation of the effective conductivity of unidirectional fibrous composites with an interfacial thermal resistance, Numer. Heat Transfer, Part A-Appl. 2001, 39(2): 179-203.
[8] Carslaw, H., Jaeger, C., Conduction of heat in solids, Clarendon Press, Oxford, 1947.
[9] Donato, P., Monsurro, S., Homogenization of two heat conductors with an interfacial contact resistance, Anal. Appl., 2004, 2(03): 247-273.
[10] Jose, E., Homogenization of a parabolic problem with an imperfect interface, Rev. Roumaine Math. Pures Appl., 2009, 54(3): 189-222.
[11] Dorfler, M., Maier, M., An elliptic problem with strongly nonlinear interface condition, Appl. Anal., 2018: 1-17.
[12] Jo, G., Kwak, D. Y., Enriched-conforming methods for elliptic interface problems with implicit jump conditions, Adv. Math. Phys., 2018.
[13] Donato,P., Some corrector results for composites with imperfect interface, Rend. Mat. Appl., VII. Ser., 2006, 26: 189-209.
[14] Beyer, R., LeVeque, R., Analysis of a one-dimensional model for the immersed boundary method, SIAM J. Numer. Anal., 1992, 29: 332-364.
[15] LeVeque, J., Lin, Z., The immersed interface method for elliptic equations with discontinuous coefficients and singular sources, SIAM J. Numer. Anal., 1994, 31: 1019-1044.
[16] Li, Z., Ito, K., Maximum principle preserving schemes for interface problems, J. Sci. Comput., 2001, 23: 339-361
[17] Li, Z., Ito,K., The immersed interface method: numerical solutions of PDEs involving interfaces and irregular domains, SIAM, Philadelphia, 2006.
[18] Wiegmann, A., and Bube,K., The immersed interface method for nonlinear differential equations with discontinuous coefficients and singular sources, SIAM J. Numer. Anal., 1998, 35: 177-200.
[19] Huang, H., Li, Z., Convergence analysis of the immersed interface method, IMA J. Numer. Anal., 1999, 19: 583-608.
[20] Thomas B. J. , Uniform error estimates for Navier-Stokes flow with an exact moving boundary using the immersed interface method, SIAM J. Numer. Anal., 2015,53(4): 2097-2111.
[21] Wiegmann, A., and Bube, K., The immersed interface method for nonlinear differential equations with discontinuous coefficients and singular sources, SIAM J. Numer. Anal., 1998, 35: 177-200.
[22] Brehm, C., Fasel,H. F., A novel concept for the design of immersed interface methods, J. Comput. Phys., 2013, 242: 234-267.
[23] Mittal, H., Ray,R., Solving immersed interface problems using a new interfacial points-based finite difference approach, SIAM J. Sci. Comput., 2018, 40(3): A1860-A1883.
[24] Cao, W., Zhang, X., Zhang, Z., et al. Superconvergence of immersed finite volume methods for one-dimensional interface problems, J. Sci. Comput., 2017, 73(2-3): 543-565.
[25] Wang, Q., Zhang, Z., A modified immersed volume element method for elliptic interface problems, ANZIAM Journal, 2020, 62(1):42-61.
[26] Costa, R., Nóbrega, J. M., Clain, S., et al. Very high-order accurate polygonal mesh finite volume scheme for conjugate heat transfer problems with curved interfaces and imperfect contacts, Comput. Methods Appl. Mech. Engrg., 2019, 357: 112560.
[27] He, X., Lin, T., Lin, Y., The convergence of the bilinear and linear immersed finite element solutions to interface problems, Numer. Methods for Partial Differ. Eq., 2012,28(1): 312-330.
[28] He, X., Lin, T., Lin, Y., Zhang, X., Immersed finite element methods for parabolic equations with moving interface, Numer. Methods for Partial Differ. Eq., 2013, 29(2): 619-646.
[29] Xu, Z., Lin, Y., Lin, T., A method of lines based on immersed finite elements for parabolic moving interface problems, Adv. Appl. Math. Mech. 2013, 5(4):548-568.
[30] He, X., Lin, T., Lin, Y., A selective immersed discontinuous Galerkin method for elliptic interface problems, Math. Methods Appl. Sci., 2014, 37(7): 983-1002.
[31] Feng, W., He, X., Lin, Y., Zhang, X., Immersed finite element method for interface problems with algebraic multigrid solver, Commun. Comput. Phys., 2014, 15(4): 1045-1067.
[32] Guo, R., Lin, T., Zhang, X., Nonconforming immersed finite element spaces for elliptic interface problems, Comput. Math. Appl., 2018, 75(6): 2002-2016.
[33] Lin, T., Sheen, D., Zhang, X., A nonconforming immersed finite element method for elliptic interface problems. J. Sci. Comput., 2019, 79(1): 442-463.

[34] He, X., Lin, T., Lin, Y., Immersed finite element methods for elliptic interface problems with non-homogeneous jump conditions, Int. J. Numer. Anal. Model., 2011, 8(2): 284-301.
[35] Lin, T., Lin, Y., Sun, W.-W., Wang, Z., Immersed finite element methods for 4-th order differential equations, J. Comput. Appl. Math., 2011, 235, 13(1): 953-3964.
[36] Wang, L., Hou, S., Shi, L., A simple FEM for solving two-dimensional diffusion equation with nonlinear interface jump conditions, CMES-Comput. Model. Engrg. Sci., 2019, 119(1): 73-90.
[37] Guo, R., Lin, T., A higher degree immersed finite element method based on a cauchy extension for elliptic interface problems, SIAM J. Numer. Anal., 2019, 57(4): 1545-1573.
[38] Guo, R., Lin, T., Lin, Y., A fixed mesh method with immersed finite elements for solving interface inverse problems, J. Sci. Comput., 2019, 79: 148-175.
[39] Guo, R., Lin, T., Lin, Y., Recovering elastic inclusions by shape optimization methods with immersed finite elements, J. Comput. Phys., 2019, 404: 109123.
[40] Guo, R., Lin, T., A trilinear immersed finite element method for solving elliptic interface problems, Numer. Anal., 2019, https://arxiv.org/abs/1905.10012.
[41] Guo, R., Lin, T., An immersed finite element method for elliptic interface problems in three dimensions, J. Comput. Phys., 2020, 414, 109478.
[42] Gong, Y., Li, Z., Immersed interface finite element methods for elasticity interface problems with non-homogeneous jump conditions, Numer. Math. Theory Methods Appl., 2010, 3 (1): 23-39.
[43] Li, Z., Yang, X., An immersed finite element method for elasticity equations with interfaces, Contemp. Math, Amer. Math. Soc., 2015, 383:285-298.
[44] Lin, T., Zhang, X., Linear and bilinear immersed finite elements for planar elasticity interface problems, J. Comput. Appl. Math., 2012, 236(18): 4681-4699.
[45] Lin, T., Sheen, D., Zhang, X., A locking-free immersed finite element method for planar elasticity interface problems, J. Comput. Phys., 2013, 247(16): 228-247.
[46] Lin, T., Yang, Q., Zhang, X., A priori error estimates for some discontinuous Galerkin immersed finite element methods, J. Sci. Comput., 2016, 65: 875-894.
[47] Lin, T., Lin, Y., Zhuang, Q., Solving interface problems of the Helmholtz equation by immersed finite element methods, Commun. Appl. Math. Comput., 2019, 1:187-206.
[48] Lin, T., Lin, Y., Sun, W.-W., Error estimation of a class of quadratic immersed finite element method for elliptic interface problems, Discrete Contin. Dyn. Syst. Ser. B, 2007, 7(4): 807-823.
[49] Lin, T., Lin, Y., and Zhang, X., Partially penalized immersed finite element methods for elliptic interface problems, SIAM J. Numer. Anal., 2015, 53(2):1121-1144
[50] Lin, T., Lin, Y., and Zhang, X., Partially penalized immersed finite element methods for parabolic interface problems, Numer. Methods for Partial. Differ. Eq., 2015, 31(6):1925-1947.
[51] Yang, Q., Numerical analysis of partially penalized immersed finite element methods for hyperbolic interface problems, Numer. Math. Theor. Methods Appl., 2018, 11: 272-298.
[52] Guo, R., Lin, T., Zhuang, Q., An improved error estimation for partially penalized immersed finite element methods for elliptic interface problems, Int. J. Numer. Anal. Model., 2019, 16(4): 575-589.
[53] Guo, R., Lin, T., Lin, Y., Approximation capabilities of immersed finite element spaces for elasticity Interface problems, Numer. Methods for Partial Differ. Eq., 2019, 35(3):1243-1268.
[54] Adjerid, S., Lin, T., Zhuang, Q., Error Estimates for an immersed finite element method for second order hyperbolic equations in inhomogeneous media, J. Sci. Comput., 2020, 84(2),https://doi.org/10.1007/s10915-020-01283-0
[55] Adjerid, S., Babuska, I., Guo, R., Lin, T., An enriched immersed finite element method for interface problems with nonhomogeneous jump conditions, Numer. Anal., 2020, https://arxiv.org/abs/2004.13244.
[56] Han, D., Wang, P., He, X., Lin, T., Wang, J., A 3D immersed finite element method with non-homogeneous interface flux jump for applications in particle-in-cell simulations of plasma-lunar surface interactions, J. Comput. Phys., 2016, 321: 965-980.
[57] Chernogorova, T., Ewing, R. E., Iliev, O., and Lazarov, R., On the discretization of interface problems with perfect and imperfect contact, Lecture Notes in Physics, New York, Spinger-Verlag, 2000, 552: 93-103.
[58] Cao, F.J., Sheng, Z.Q., Yuan, G.W., Monotone finite volume schemes for diffusion equation with imperfect interface on distorted meshes, J. Sci. Comput., 2018, 76(2): 1055-1077.
[59] Zhou, H., Sheng, Z., Yuan, G., A finite volume method preserving maximum principle for the diffusion equations with imperfect interface. Appl. Numer. Math., 2020, 158: 314-335.

[60] Morton, K. W., and Mayers, D. F., Numerical solution of partial differential equations, Cambridge: Cambridge University Press, 1995.

School of Science, Inner Mongolia University of Science and Technology ,Baotou 014010,Inner Mongolia, P. R. China
E-mail: caofujun@imust.edu.cn and yuandf@imust.edu.cn

Laboratory of Computational Physics, Institute of Applied Physics and Computational Mathematics, P. O. Box 8009, Beijing 100088, P. R. China
E-mail: sheng_zhiqiang@iapcm.ac.cn and yuan_guangwei@iapcm.ac.cn

School of Science, Inner Mongolia University of Science and Technology ,Baotou 014010,Inner Mongolia, P. R. China
E-mail: helimin2003@163.com